Dual frequency comb spectroscopy with a single laser

I. Znakovskaya,[1,2] E. Fill,[1,2,*] N. Forget,[3] P. Tournois,[3] M. Seidel,[2] O. Pronin,[1] F. Krausz,[1,2] and A. Apolonski[1,2]

[1]Ludwig-Maximilians-Universität München, Am Coulombwall 1, D-85748 Garching, Germany

[2]Max-Planck-Institut für Quantenoptik, Hans-Kopfermann-Str. 1, D-85748 Garching, Germany

[3]Fastlite, 1900 route des crêtes, 06560 Valbonne, France

*Corresponding author: ernst.fill@mpq.mpg.de

Received July 1, 2014; accepted August 6, 2014;
posted August 20, 2014 (Doc. ID 214273); published September 16, 2014

We demonstrate a simple scheme for dual frequency comb spectroscopy in which the second frequency comb is generated by propagating the primary pulse train through a dazzler. The two frequency combs are combined behind a Mach–Zehnder interferometer, and the optical spectrum is read out by an rf-spectrum analyzer. The method is applied to record the overtone absorption spectrum of C_2H_2 (acetylene) in the wavelength region around 1.03 μm. A spectrum with a resolution of 4 cm^{-1} is obtained, which compares well with that from the HITRAN database. A simple method for improving the spectral resolution is demonstrated. © 2014 Optical Society of America

OCIS codes: (300.6300) Spectroscopy, Fourier transforms; (300.6310) Spectroscopy, heterodyne; (300.6340) Spectroscopy, infrared; (320.7090) Ultrafast lasers.

http://dx.doi.org/10.1364/OL.39.005471

Dual frequency comb spectroscopy (DFCS) is a powerful technique for rapid recording of broadband spectra [1–6]. It is similar to Fourier-transform spectroscopy but without moving parts. Applied to the infrared region, its speed and accuracy make it a very valuable tool for trace gas detection, breath analysis, and environmental control [7–9].

DFCS utilizes two mode-locked femtosecond lasers with slightly different repetition rates. Each line of the primary frequency comb is characterized by its specific beat frequency with the corresponding line of the second comb. In this way, the optical spectrum is transferred into the rf region. DFCS can be realized by combining the combs before the sample (as done here), in which case the intensity absorption spectrum is recorded. Alternatively the combs can be combined after the sample, yielding both the magnitude and phase spectrum [6].

A basic problem of DFCS is that the amplitudes and repetition rates of the two lasers have to be well-stabilized to avoid degrading the spectrum [10]. In recent implementations the required stability has been achieved by locking individual lines of both combs to two ultrastable cw lasers [4], or by deriving adaptive phase correction signals from the two cw lasers [11]. Both methods, however, require four lasers for their realization.

An alternative method for producing a dual frequency comb uses two Mach–Zehnder modulators for generating rf sidebands of a cw laser. In this way frequency combs containing up to 50 frequency components and spanning a bandwidth of 200 GHz were realized [12].

In this Letter we demonstrate a scheme for DFCS in which the second frequency comb is generated by propagating the primary pulse train through an acousto-optic programmable dispersive filter (AOPDF, henceforth called dazzler [13]). Thus, only a single femtosecond laser is needed, and the repetition rates and amplitudes of the two combs are automatically stabilized with high precision.

A dazzler is a universal device which can be used to manipulate ultrashort pulses. It can be applied for chirp compensation, pulse shaping, and spectral filtering [14–16]. Moreover, irradiated by a pulse train with multi-MHz repetition rate the dazzler generates another pulse train with a slightly different repetition rate. The second pulse train is locked to the first one with high accuracy. This remarkable property has recently been used to demonstrate asynchronous optical sampling with a precision of 15 as [17].

The main component of a dazzler is a birefringent crystal, in which an acoustic pulse propagates collinearly with the laser beam (parallel Poynting vectors). The primary laser pulse train propagates as an ordinary ray in the crystal. The sound wave diffracts part of its power into a second pulse train propagating as an extraordinary ray. In the crystal used here (TeO_2) extraordinary rays exhibit a slightly lower group velocity, and thus these pulses are temporally delayed with respect to the primary pulses. As the acoustic pulse propagates the acousto-optic diffraction occurs at different penetration depths, and the delay of the second pulse train decreases linearly in time with respect to the primary pulse train. The difference in group velocities and the different propagation distances in the crystal result in an incremental delay of the diffracted pulses given by [16,17]

$$\Delta t = t_{\mathrm{rep}}\left(n_{g,e} - n_{g,o}\right)V/c = \mu t_{\mathrm{rep}}. \tag{1}$$

In Eq. (1) t_{rep} is the roundtrip time of the primary pulse train (the inverse of the repetition frequency f_{rep}); $n_{g,e}$ and $n_{g,o}$ are the group velocity indices of the extraordinary and the ordinary rays, respectively; V is the sound velocity; and c the velocity of light. The parameter $\mu = (n_{g,e}–n_{g,o})\mathrm{V/c}$ in Eq. (1) is a dimensionless constant of the dazzler. Its value depends on the dazzler material and the crystallographic orientation of the crystal. Using known material constants a fairly accurate value for μ can be found. However, its value can be refined by calibrating it with accurately known lines in the spectrum (discussed in a subsequent paragraph). For the device used in the research reported in this Letter, the numerical value derived in this way was $\mu = 2.5 \times 10^{-7}$. At our repetition rate of 38 MHz the incremental time delay Δt is thus 6.6 fs.

With $\Delta t > 0$ the diffracted pulse train has a slightly lower repetition rate, and thus generates a frequency comb with slightly smaller comb line spacing. The difference is

$$\Delta f_{\mathrm{rep}} = -\mu f_{\mathrm{rep}}, \tag{2}$$

and thus in our experiment the change in repetition rate and comb line spacing is –9.5 Hz.

The beat frequencies measured by the spectrum analyzer include contributions from the acoustic Doppler shift of the secondary frequency comb, $f_{\mathrm{ac}} = 64.9$ MHz, and the difference Δf_{ceo} in the carrier envelope frequencies of the two combs. The value of the acoustic shift is determined by the requirement of phase matching between optical and sound waves. The value of Δf_{ceo} is related to the different group and phase velocities of the two pulse trains. Thus, at an optical frequency ν_{opt} the shift of a secondary comb line with respect to the corresponding primary one is given by

$$\begin{aligned} f_{\mathrm{shift}} &= f_{\mathrm{ac}} + \Delta f_{\mathrm{ceo}} + V_{\mathrm{opt}} \Delta f_{\mathrm{rep}}/f_{\mathrm{rep}} \\ &= f_{\mathrm{ac}} + \Delta f_{\mathrm{ceo}} - \mu V_{\mathrm{opt}}. \end{aligned} \tag{3}$$

Since the secondary frequency comb also beats with other primary comb lines we see beat frequencies at $f_{\mathrm{beat}} = |f_{\mathrm{shift}} \pm N_0 f_{\mathrm{rep}}|$, where N_0 is an integer including zero.

For the experiment a Kerr-lens mode-locked thin disk Yb:YAG oscillator emitting 250 fs pulses at a repetition rate of $f_{\mathrm{rep}} = 38$ MHz was used as the light source [18]. The spectrum is centered at $\lambda_c = 1030$ nm with a FWHM of 4.5 nm. While this laser is capable of emitting a power of up to 40 W, only about 2 W were utilized. This power level was required to achieve sufficient broadening of the spectrum in the fiber. The power reaching the detector was about 100 mW.

The lowest beat frequencies observed are at 11, 27, 49, and 65 MHz. We used the region around the 11 MHz beat frequency for evaluating the spectra, taking into account that for this frequency ($N_0 = 0$, thus $f_{\mathrm{beat}} = f_{\mathrm{shift}}$) higher rf frequencies correspond to lower optical frequencies.

The sound pulse traverses the 25 mm long dazzler crystal in a time $t_{\mathrm{trans}} = 33$ μs. After a short dead time another sound pulse is launched. Thus the secondary pulse train consists of about 1,000 laser pulses, and the comb lines of the secondary frequency comb are broadened by $1/t_{\mathrm{trans}} = 30$ kHz. This results in a spectral resolution of approximately $1/(\mu t_{\mathrm{trans}}) = 0.12$ THz, corresponding to 4 cm^{-1}.

Acetylene has two overtone absorption bands in the wavelength range 1.01–1.045 μm [19]. To cover this region, the spectrum of the laser was broadened to about 35 nm by focusing it into an LMA-35 photonic crystal fiber. After collimation the pulses were sent to a stage of dispersive mirrors for partial chirp compensation.

Figure 1 shows the setup of the spectrometer. The dazzler was incorporated into one arm of a Mach–Zehnder interferometer. This was necessary since the two pulse trains leave the dazzler under a slightly different angle, and therefore cannot directly interfere on a detector. A movable delay line was placed in the other arm of the interferometer. It compensates the optical delay of the pulses in the dazzler and allows positioning the region in which the pulses overlap (the so-called centerburst) anywhere in the interferogram. The output of the interferometer was passed through a 26 cm long absorption cell which could be pressurized up to 2.5 bar. A Si diode behind the cell recorded the pulses. The interferogram was recorded by an oscilloscope, and the optical spectrum was directly read out by an rf-spectrum analyzer.

Figure 2 shows an interferogram in which the centerburst is moved to the left corner. The centerburst is an undersampled first-order autocorrelation of the laser spectrum. Narrow absorption features are contained in the plateau following the centerburst. Figure 3 shows the measured transmittance of acetylene (purity 99.2%) at a pressure of 2.4 bar, obtained by dividing the spectrum analyzer signal with the gas-filled cell by that of the empty cell. The spectrum analyzer resolution was 1 kHz, and the data were averaged over 500 interferograms.

Figure 4 shows the spectral absorption coefficient of 2.4 bar acetylene derived from the transmittance. Realizing that the frequency in Fig. 3 is the fundamental beat frequency f_{shift}, it follows from Eq. (3) that the wavelength scale is given by $\lambda(\mu\mathrm{m}) = 10^4 c\mu/(f_{\mathrm{ac}} + \Delta f_{\mathrm{ceo}} - f)$, where c is in cm/s and all frequencies are in Hertz. As

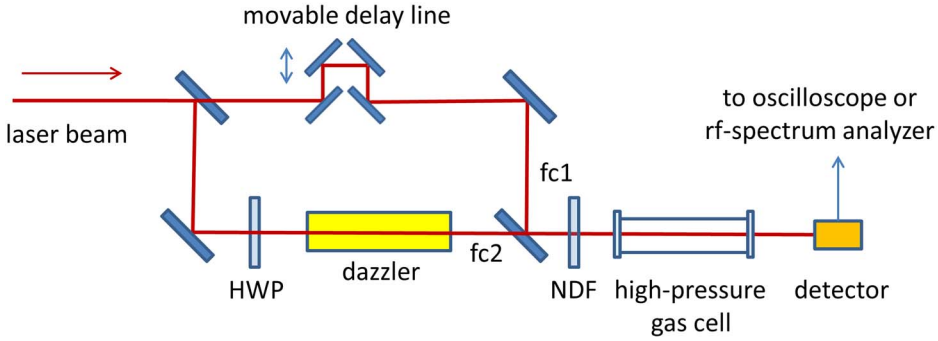

Fig. 1. Experimental arrangement for DFCS with a single laser. Spectrally broadened laser pulses are input to a Mach–Zehnder interferometer containing the dazzler in one arm, and a movable delay line in the other. HWP, half wave plate, for rotating the plane of polarization of the arm containing the dazzler by 90°; NDF, neutral density filter, to avoid saturating the detector. The two frequency combs fc1 and fc2 are combined after the interferometer, and passed through a high-pressure gas cell. Interferograms are read out by means of an oscilloscope, and optical spectra by an rf-spectrum analyzer.

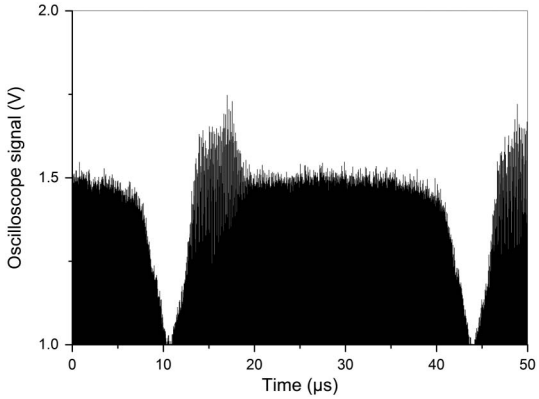

Fig. 2. Interferogram as recorded by the oscilloscope. Interferograms repeat each other at a rate of 30 kHz set by the frequency at which sound pulses are launched. The peak on the left is the pulse overlap region, the so-called centerburst. It is a first-order autocorrelation of the laser spectrum. Gas absorption features are contained in the plateau following the centerburst (the region 20–40 μs).

mentioned previously, the values of $\mu = 2.5 \times 10^{-7}$ and of $\Delta f_{\mathrm{ceo}} = 19$ MHz are obtained by matching data points of the experimental spectrum with the corresponding wavelengths from the HITRAN database [20]. The HITRAN spectrum, smoothed to take a resolution of 4 cm^{-1} into account, is included for comparison. Good agreement between the two is found.

In a further experiment an attempt was made to improve the spectral resolution. For this purpose the centerburst of the interferogram was moved out of the recorded region by an appropriate movement of the delay line in the interferometer. In this way the plateau of the interferogram, which contains the absorption lines, is extended to higher Fourier frequencies.

Figure 5 shows the result, which indeed exhibits an improved resolution of about 2 cm^{-1}. We note, however, that moving the centerburst out of the interferogram is equivalent to filtering the spectrum with a high-frequency window. Therefore, the spectrum is distorted and gross features are lost.

In conclusion, a simple technique for DFCS is demonstrated which requires only a single laser. A dazzler

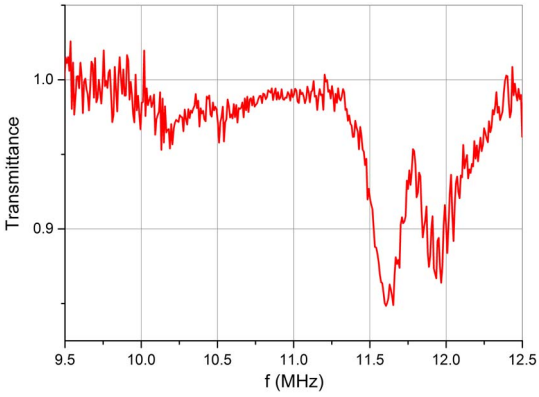

Fig. 3. Transmittance of 2.4 bar of acetylene through a 26 cm absorption cell versus rf frequency. Note that for this beat frequency region, higher rf frequencies correspond to lower optical frequencies.

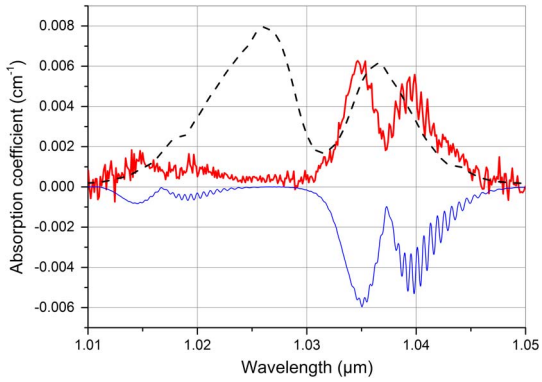

Fig. 4. Absorption coefficient of 2.4 bar acetylene (C_2H_2) as measured by transmission through a 26 cm long absorption cell. The upper trace in red is our data, which are compared to the HITRAN database (blue, shown negative). The HITRAN data have been smoothed to take a resolution of 4 cm^{-1} into account. The dashed line is the spectrum of the laser.

generates the second frequency comb exactly synchronized with the primary one. The comb beating frequencies are directly read out by an rf-spectrum analyzer.

In further experiments this technique can be improved with regard to resolution and sensitivity. A straightforward way to increase the resolution involves using a longer dazzler crystal. As demonstrated, higher resolution can also be obtained by moving the centerburst out of the recorded interferogram. This procedure is equivalent to applying a high-pass filter to the spectrum, and therefore the improvement comes at the expense of some distortion of the spectrum.

Additional progress relates to the sensitivity of the dazzler spectrometer. By autobalanced detection [21] laser noise can be reduced by a large factor, resulting in shot-noise limited operation with dramatically increased sensitivity [22].

Finally, it may be mentioned that the high repetition rate of dazzler operation (up to 40 kHz) allows time-resolved studies.

This Letter was funded by the DFG Cluster of Excellence "Munich Centre for Advanced Photonics" (MAP; www.munich.photonics.de). The authors acknowledge the

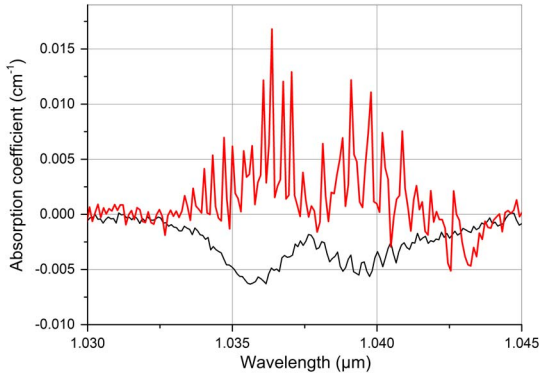

Fig. 5. Spectrum with higher resolution obtained by moving the centerburst out of the interferogram (upper trace). Higher-resolution data are obtained with an acetylene pressure of 1.6 bar. Data obtained with the centerburst in the left corner of the interferogram (as in Fig. 2) are displayed negative for comparison.

technical help of L. Lötscher and M. Kübel, as well as discussions with F. Keilmann.

References

1. F. Keilmann, C. Gohle, and R. Holzwarth, Opt. Lett. **29**, 1542 (2004).
2. A. Schliesser, M. Brehm, F. Keilmann, and D. W. van der Weide, Opt. Express **13**, 9029 (2005).
3. S. Schiller, Opt. Lett. **27**, 766 (2002).
4. I. Coddington, W. C. Swann, and N. R. Newbury, Phys. Rev. Lett. **100**, 013902 (2008).
5. B. Bernhardt, A. Ozawa, P. Jaquet, M. Jacquey, Y. Kobayashi, T. Udem, R. Holzwarth, G. Guelachvili, Th. Hänsch, and N. Piqué, Nat. Photonics **4**, 55 (2009).
6. I. Coddington, W. C. Swann, and N. R. Newbury, Phys. Rev. A **82**, 043817 (2010).
7. S. Diddams, L. Hollberg, and V. Mbele, Nature **445**, 627 (2007).
8. M. J. Thorpe and J. Ye, Appl. Phys. B **91**, 397 (2008).
9. M. J. Thorpe, D. Balslev-Clausen, M. S. Kirchner, and J. Ye, Opt. Express **16**, 2387 (2008).
10. N. R. Newbury, I. Coddington, and W. C. Swann, Opt. Express **18**, 7929 (2010).
11. T. Ideguchi, A. Poisson, G. Guelachvili, N. Piqué, and T. W. Hänsch, Nat. Commun. **5**, 3375 (2014).
12. D. A. Long, A. J. Fleisher, K. O. Douglass, S. E. Maxwell, K. Bielska, J. T. Hodges, and F. Plusquellic, Opt. Lett. **39**, 2688 (2014).
13. http://www.fastlite.com/.
14. P. Tournois, Opt. Commun. **140**, 245 (1997).
15. F. Verluise, V. Laude, Z. Cheng, Ch. Spielmann, and P. Tournois, Opt. Lett. **25**, 575 (2000).
16. F. Verluise, V. Laude, J.-P. Huignard, P. Tournois, and A. Migus, J. Opt. Soc. Am. B **17**, 138 (2000).
17. O. Schubert, M. Eisele, V. Crozatier, N. Forget, D. Kaplan, and R. Huber, Opt. Lett. **38**, 2907 (2013).
18. O. Pronin, J. Brons, C. Grasse, V. Pervak, G. Boehm, M.-C. Amann, V. L. Kalashnikov, A. Apolonski, and F. Krausz, Opt. Lett. **36**, 4746 (2011).
19. D. Jacquemart, N. Lacome, and J.-Y. Mandin, J. Quant. Spectrosc. Radiat. Transfer **110**, 733 (2009).
20. L. S. Rothman, I. E. Gordon, Y. Babikov, A. Barbe, D. C. Benner, P. F. Bernath, M. Birk, L. Bizzocchi, V. Boudon, L. R. Brown, A. Campargue, K. Chance, E. A. Cohen, L. H. Coudert, V. M. Devi, B. J. Drouin, A. Fayt, J.-M. Flaud, R. R. Gamachem, J. J. Harrison, J.-M. Hartmann, C. Hill, J. T. Hodges, D. Jacquemart, A. Jolly, J. Lamouroux, R. J. LeRoy, G. Li, D. A. Long, O. M. Lyulin, C. J. Mackie, S. T. Massie, S. Mikhailenko, H. S. P. Müller, O. V. Naumenko, A. V. Nikitin, J. Orphal, V. Perevalov, A. Perrin, E. R. Polovtseva, C. Richard, M. A. H. Smith, E. Starikova, K. Sung, S. Tashkun, J. Tennyson, G. C. Toon, Vl. G. Tyuterev, and G. Wagner, J. Quant. Spectrosc. Radiat. Transfer **110**, 533 (2009)
21. P. C. D. Hobbs, Appl. Opt. **36**, 903 (1997).
22. A. Foltynowicz, T. Ban, P. Maslowski, F. Adler, and J. Ye, Phys. Rev. Lett. **107**, 233002 (2011).